Proceedings of the 38th
Conference on Decision & Control
Phoenix, Arizona USA • December 1999

Proposal of Perfect Tracking and Perfect Disturbance Rejection Control by Multirate Sampling and Applications to Hard Disk Drive Control

Hiroshi Fujimoto Yoichi Hori

Dept. Electrical Eng., Univ. of Tokyo
2-11-16 Yayoi, Bunkyo, Tokyo, 113-8656 Japan
{fuji, hori}@hori.t.u-tokyo.ac.jp

Takashi Yamaguchi Shinsuke Nakagawa

Mech. Eng. Research Lab., Hitachi, Ltd.
502 Kandatsu, Tsuchiura, 300-0013, Japan
{tkyamagu, naks}@merl.hitachi.co.jp

Abstract

In this paper, new multirate two-degree-of-freedom controllers are proposed for digital control systems, where it is restricted that the speed of the A/D converters are slower than that of the D/A converters. The proposed feedforward controller assures the perfect tracking at M inter-sampling points. Moreover, the proposed feedback controller assures the perfect disturbance rejection at M inter-sample points in the steady state. Illustrative examples of position control for hard disk drive are presented, and the advantages of this approach are demonstrated.

1 Introduction

A digital control system usually has two samplers for the reference signal $r(t)$ and the output $y(t)$, and one holder on the input $u(t)$ as shown in Fig. 1. Therefore, there exist three time periods T_r, T_y, and T_u which represent the period of $r(t), y(t)$, and $u(t)$, respectively. The input period T_u is generally decided by the speed of the actuator, D/A converter, or the calculation on the CPU. Moreover, the output period T_y is also determined by the speed of the sensor or the A/D converter.

In this paper, the digital control systems which have hardware restrictions of $T_u < T_y$ are assumed, and novel design methods of multirate two-degree-of-freedom (TDOF) controllers are proposed, which achieve "the perfect tracking" and "the perfect disturbance rejection" at M inter-sample points of T_y. The restriction of $T_u < T_y$ may be general because D/A converters are usually faster than the A/D converters. Especially, head-positioning systems of the hard disk drive (HDD) or the visual servo systems of robot manipulator belong to this category, because the sampling rates of the measurement are relatively slow.

[1, 2, 3, 4] have attempted to use multirate sampling controllers to HDD systems. This paper apply the proposed perfect tracking feedforward controller to the track-seeking mode of HDD, and the proposed perfect disturbance rejection controller is also applied to the track-following mode.

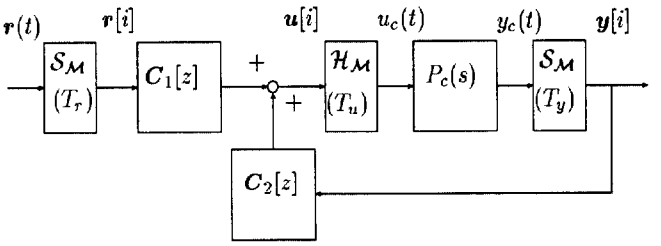

Figure 1: Two-degree-of-freedom control system.

Recently, the modern sampled-data control theories have developed, which can optimize the inter-sample response [5]. In contrast, the proposed methods make simple and practical approaches to grantee the smooth inter-sample responses by controlling all of the plant states (e.g. position and velocity) at M inter-sample points.

2 Design of the multirate TDOF controller

In this section, new multirate TDOF controllers are proposed. For the restriction of $T_u < T_y$, the flame period T_f is defined as $T_f = T_y$, and the dynamics of the controller is described by T_f.

In this paper, the integer M is selected so as to $M \triangleq N/n$ becomes an integer, where N is the input multiplicity and n is the plant order. As shown in Fig. 2, the plant input is changed N times during $T_y(= T_f)$, and the perfect tracking and the perfect disturbance rejection of the plant state are guaranteed M times during T_y.

For simplification, the continuous-time plant is assumed to be SISO system in this paper. The proposed methods, however, can be extended to deal with the MIMO system by the same way as [6].

2.1 Plant Discretization by Multirate Sampling

Consider the continuous-time plant described by

$$\dot{\boldsymbol{x}}(t) = \boldsymbol{A}_c\boldsymbol{x}(t) + \boldsymbol{b}_c u(t) \ , \quad y(t) = \boldsymbol{c}_c\boldsymbol{x}(t). \qquad (1)$$

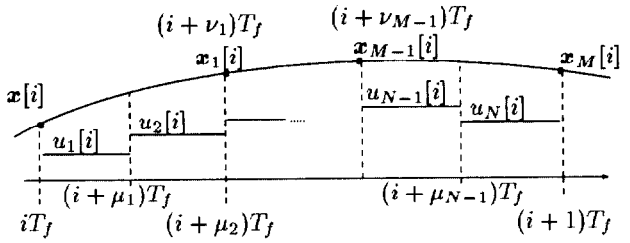

Figure 2: Multirate Sampling control.

The discrete-time plant discretized by the multirate sampling control (Fig. 2) becomes

$$\boldsymbol{x}[i+1] = \boldsymbol{A}\boldsymbol{x}[i] + \boldsymbol{B}\boldsymbol{u}[i]\ ,\quad y[i] = \boldsymbol{C}\boldsymbol{x}[i] \tag{2}$$

where $\boldsymbol{x}[i] = \boldsymbol{x}(iT)$, and where matrices $\boldsymbol{A}, \boldsymbol{B}, \boldsymbol{C}$ and vectors $\boldsymbol{u}$ are given by

$$\left[\begin{array}{c|c} \boldsymbol{A} & \boldsymbol{B} \\ \hline \boldsymbol{C} & \boldsymbol{O} \end{array}\right] \triangleq \left[\begin{array}{c|ccc} e^{\boldsymbol{A}_c T_f} & \boldsymbol{b}_1 & \cdots & \boldsymbol{b}_N \\ \hline \boldsymbol{c}_c & 0 & \cdots & 0 \end{array}\right], \tag{3}$$

$$\boldsymbol{b}_j \triangleq \int_{(1-\mu_j)T_f}^{(1-\mu_{(j-1)})T_f} e^{\boldsymbol{A}_c \tau}\boldsymbol{b}_c d\tau\ ,\ \boldsymbol{u} \triangleq [u_1, \cdots, u_N]^T, \tag{4}$$

$$0 = \mu_0 < \mu_1 < \mu_2 < \ldots < \mu_N = 1. \tag{5}$$

The inter-sample plant state at $t = (i+\nu_k)T_f$ is represented by

$$\tilde{\boldsymbol{x}}[i] = \tilde{\boldsymbol{A}}\boldsymbol{x}[i] + \tilde{\boldsymbol{B}}\boldsymbol{u}[i], \tag{6}$$

$$\left[\ \tilde{\boldsymbol{A}}\ \middle|\ \tilde{\boldsymbol{B}}\ \right] \triangleq \left[\begin{array}{c|ccc} \tilde{\boldsymbol{A}}_1 & \tilde{\boldsymbol{b}}_{11} & \cdots & \tilde{\boldsymbol{b}}_{1N} \\ \vdots & \vdots & & \vdots \\ \tilde{\boldsymbol{A}}_M & \tilde{\boldsymbol{b}}_{M1} & \cdots & \tilde{\boldsymbol{b}}_{MN} \end{array}\right], \tag{7}$$

$$\tilde{\boldsymbol{A}}_k \triangleq e^{\boldsymbol{A}_c \nu_k T_f},\ \tilde{\boldsymbol{x}} \triangleq [\boldsymbol{x}_1, \cdots, \boldsymbol{x}_M]^T \tag{8}$$

$$\boldsymbol{x}_k[i] = \boldsymbol{x}[i+\nu_k] = \boldsymbol{x}((i+\nu_k)T_f), \tag{9}$$

$$\tilde{\boldsymbol{b}}_{kj} \triangleq \left\{\begin{array}{cc} \mu_j < \nu_k : & \int_{(\nu_k-\mu_j)T_f}^{(\nu_k-\mu_{(j-1)})T_f} e^{\boldsymbol{A}_c\tau}\boldsymbol{b}_c d\tau \\ \mu_{(j-1)} < \nu_k \le \mu_j : & \int_0^{(\nu_k-\mu_{(j-1)})T_f} e^{\boldsymbol{A}_c\tau}\boldsymbol{b}_c d\tau \\ \nu_k \le \mu_{(j-1)} : & 0 \end{array}\right.,$$

$$0 < \nu_1 < \nu_2 < \ldots < \nu_M = 1. \tag{10}$$

where $\mu_j (j = 0, 1, \cdots, N)$ and $\nu_k (k = 1, \cdots, M)$ are the parameters for multirate sampling as shown in Fig. 2. If T_f is divided at same intervals, $\mu_j = j/N, \nu_k = k/M$.

2.2 Design of the perfect tracking controller

In the conventional digital tracking control systems, it is impossible to track the desired trajectory with zero error [7], because the discrete-time plant discretized by the zero-order-hold usually has unstable zeros [8].

The unstable zeros problems of the discrete-time plant have been resolved by zero assignment method in use of multirate control in [9] and [10]. However, [11] shows

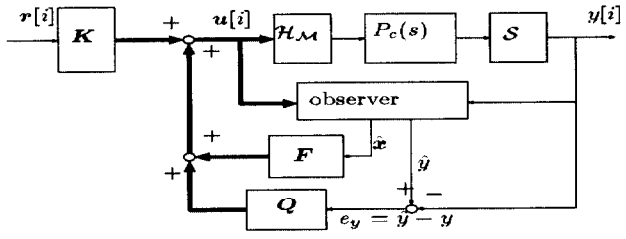

Figure 3: Basic structure of TDOF control.

that those methods have disadvantages of large overshoot and oscillation in the inter-sample points because the control input changes back and forth very quickly. On the other hand, [12] proposed the perfect tracking control by introducing the multirate feedforward control, which never has this problem because all of the plant states are controlled along the smoothed desired trajectories.

In this section, the perfect tracking controller $\boldsymbol{C}_1[z]$ is designed so that the plant state $(\boldsymbol{x})$ completely track the desired trajectory $(\boldsymbol{x}^*)$ at every sampling points $T_r (= T_y/M)$ [13].

The control law of Fig. 1 is described by

$$\boldsymbol{u} = \boldsymbol{C}_1\boldsymbol{r} + \boldsymbol{C}_2\boldsymbol{y} \tag{11}$$

$$= \boldsymbol{F}\hat{\boldsymbol{x}} + \boldsymbol{Q}\boldsymbol{e}_y + \boldsymbol{K}\boldsymbol{r} \tag{12}$$

where $\boldsymbol{K}, \boldsymbol{Q} \in \boldsymbol{RH}_\infty$ are free parameters [14]. Therefore, Fig. 1 can be transferred to Fig. 3. In the figure, $\mathcal{H}_{\mathcal{M}}$, $\mathcal{S}$, and the thick lines represent the multirate hold, the sampler, and the multirate signals, respectively. In this paper, $\boldsymbol{K}$ becomes a constant matrix.

Because the estimation errors of the observer become zero $(\hat{\boldsymbol{x}} = \boldsymbol{x}, \boldsymbol{e}_y = 0)$ for the nominal plant, from (6) and (12), this system is represented by

$$\tilde{\boldsymbol{x}}[i] = (\tilde{\boldsymbol{A}} + \tilde{\boldsymbol{B}}\boldsymbol{F})\boldsymbol{x}[i] + \tilde{\boldsymbol{B}}\boldsymbol{K}\boldsymbol{r}[i]. \tag{13}$$

[15] proved that the matrix $\tilde{\boldsymbol{B}}$ is non-singular and that the coefficient matrices of (13) can be arbitrary assigned by $\boldsymbol{F}$ and $\boldsymbol{K}$. In this paper, the parameters $\boldsymbol{F}, \boldsymbol{K}$ can be selected so that following equations are satisfied

$$\tilde{\boldsymbol{A}} + \tilde{\boldsymbol{B}}\boldsymbol{F} = \boldsymbol{O}\ ,\quad \tilde{\boldsymbol{B}}\boldsymbol{K} = \boldsymbol{I}. \tag{14}$$

From (14), $\boldsymbol{F}, \boldsymbol{K}$ are given by

$$\boldsymbol{F} = -\tilde{\boldsymbol{B}}^{-1}\tilde{\boldsymbol{A}}\ ,\quad \boldsymbol{K} = \tilde{\boldsymbol{B}}^{-1}. \tag{15}$$

Therefore, (13) is described by $\tilde{\boldsymbol{x}}[i] = \boldsymbol{r}[i]$. Utilizing the inter-sample desired state $\tilde{\boldsymbol{x}}^*[i]$, if the reference input is set to $\boldsymbol{r}[i] = \tilde{\boldsymbol{x}}^*[i]$, we find the perfect tracking $\tilde{\boldsymbol{x}}[i] = \tilde{\boldsymbol{x}}^*[i]$ can be achieved at every sampling point T_r.

Because $\boldsymbol{C}_1[z]$ of (11) can be transferred to (16), $\boldsymbol{C}_1[z]$ is given by (Fig. 4)

$$\boldsymbol{C}_1[z] = (\boldsymbol{M} - \boldsymbol{C}_2\boldsymbol{N})\boldsymbol{K}, \tag{16}$$

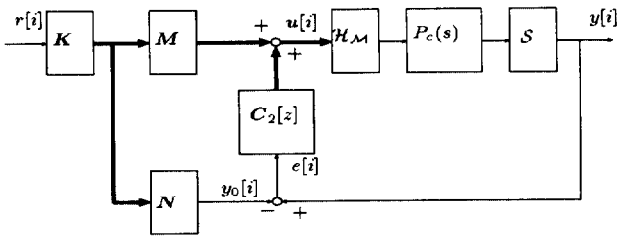

Figure 4: Implementation of the proposed controller.

$$\begin{aligned} \boldsymbol{M} &= \left[\begin{array}{c|c} \boldsymbol{A}+\boldsymbol{BF} & \boldsymbol{B} \\ \hline \boldsymbol{F} & \boldsymbol{I} \end{array}\right] = \boldsymbol{I} + z^{-1}\boldsymbol{FB}, \\ \boldsymbol{N} &= \left[\begin{array}{c|c} \boldsymbol{A}+\boldsymbol{BF} & \boldsymbol{B} \\ \hline \boldsymbol{C} & \boldsymbol{O} \end{array}\right] = z^{-1}\boldsymbol{CB}, \end{aligned} \tag{17}$$

where $\boldsymbol{M}, \boldsymbol{N}$ are the right coprime factorization of the plant $\boldsymbol{P}[z] = \boldsymbol{NM}^{-1}$[16].

2.3 Design of the perfect disturbance rejection controller

In this section, new multirate feedback controller is proposed based on the state space design of the disturbance observer.

Consider the continuous-time plant model described by

$$\dot{\boldsymbol{x}}_p(t) = \boldsymbol{A}_{cp}\boldsymbol{x}_p(t) + \boldsymbol{b}_{cp}(u(t) - d(t)) \tag{18}$$

$$y(t) = \boldsymbol{c}_{cp}\boldsymbol{x}_p(t), \tag{19}$$

where $d(t)$ is the disturbance input. Let the disturbance model be

$$\dot{\boldsymbol{x}}_d(t) = \boldsymbol{A}_{cd}\boldsymbol{x}_d(t)\ ,\ d(t) = \boldsymbol{c}_{cd}\boldsymbol{x}_d(t). \tag{20}$$

For example, the step type disturbance can be modeled by $\boldsymbol{A}_{cd} = 0, \boldsymbol{c}_{cd} = 1$. The continuous-time augmented system consisting of (18) and (20) is represented by

$$\dot{\boldsymbol{x}}(t) = \boldsymbol{A}_c\boldsymbol{x}(t) + \boldsymbol{b}_c u(t) \tag{21}$$

$$y(t) = \boldsymbol{c}_c\boldsymbol{x}(t) \tag{22}$$

$$\boldsymbol{A}_c \triangleq \begin{bmatrix} \boldsymbol{A}_{cp} & -\boldsymbol{b}_{cp}\boldsymbol{c}_{cd} \\ \boldsymbol{O} & \boldsymbol{A}_{cd} \end{bmatrix}, \boldsymbol{b}_c \triangleq \begin{bmatrix} \boldsymbol{b}_{cp} \\ 0 \end{bmatrix}, \boldsymbol{x} \triangleq \begin{bmatrix} \boldsymbol{x}_p \\ \boldsymbol{x}_d \end{bmatrix}$$

$$\boldsymbol{c}_c \triangleq [\boldsymbol{c}_{cp}, 0].$$

Discretizing (21) by the multirate sampling control, the inter-sample plant state at $t = (i+\nu_k)T_f$ can be calculated from the kth row of (6) by

$$\boldsymbol{x}[i+\nu_k] = \tilde{\boldsymbol{A}}_k\boldsymbol{x}[i] + \tilde{\boldsymbol{B}}_k\boldsymbol{u}[i] \tag{23}$$

$$\tilde{\boldsymbol{A}}_k = \begin{bmatrix} \tilde{\boldsymbol{A}}_{pk} & \tilde{\boldsymbol{A}}_{pdk} \\ \boldsymbol{O} & \tilde{\boldsymbol{A}}_{dk} \end{bmatrix}, \tilde{\boldsymbol{B}}_k = \begin{bmatrix} \tilde{\boldsymbol{B}}_{pk} \\ \boldsymbol{O} \end{bmatrix}.$$

For the plant (21) discretized by (2), the discrete-time observer on the sampling points is obtained from the Gopinath's method by

$$\hat{\boldsymbol{v}}[i+1] = \hat{\boldsymbol{A}}\hat{\boldsymbol{v}}[i] + \hat{\boldsymbol{b}}\boldsymbol{y}[i] + \hat{\boldsymbol{J}}\boldsymbol{u}[i] \tag{24}$$

$$\hat{\boldsymbol{x}}[i] = \hat{\boldsymbol{C}}\hat{\boldsymbol{v}}[i] + \hat{\boldsymbol{d}}\boldsymbol{y}[i]. \tag{25}$$

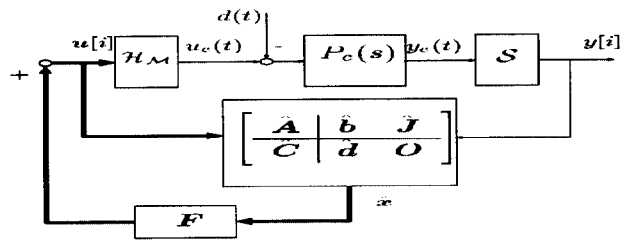

Figure 5: Multirate control with disturbance observer.

As shown in Fig. 5, let the feedback control law be

$$\boldsymbol{u}[i] = \boldsymbol{F}_p\hat{\boldsymbol{x}}_p[i] + \boldsymbol{F}_d\hat{\boldsymbol{x}}_d[i] = \boldsymbol{F}\hat{\boldsymbol{x}}[i], \tag{26}$$

where $\boldsymbol{F} \triangleq [\boldsymbol{F}_p, \boldsymbol{F}_d]$. Notice that the $\boldsymbol{F}$ of the above equation is different from that of (12) used in $\boldsymbol{C}_1[z]$ design. Letting $\boldsymbol{e}_v$ be the estimation errors of the observer ($\boldsymbol{e}_v = \hat{\boldsymbol{v}} - \boldsymbol{v}$), the following equation is obtained.

$$\hat{\boldsymbol{x}}[i] = \boldsymbol{x}[i] + \hat{\boldsymbol{C}}\boldsymbol{e}_v[i]. \tag{27}$$

From (23) to (27), the closed-loop system is represented by

$$\begin{bmatrix} \boldsymbol{x}_p[i+\nu_k] \\ \boldsymbol{x}_d[i+\nu_k] \\ \boldsymbol{e}_v[i+1] \end{bmatrix} = \tag{28}$$

$$\begin{bmatrix} \tilde{\boldsymbol{A}}_{pk} + \tilde{\boldsymbol{B}}_{pk}\boldsymbol{F}_p & \tilde{\boldsymbol{A}}_{pdk} + \tilde{\boldsymbol{B}}_{pk}\boldsymbol{F}_d & \tilde{\boldsymbol{B}}_{pk}\boldsymbol{F}\hat{\boldsymbol{C}} \\ \boldsymbol{O} & \tilde{\boldsymbol{A}}_{dk} & \boldsymbol{O} \\ \boldsymbol{O} & \boldsymbol{O} & \hat{\boldsymbol{A}} \end{bmatrix} \begin{bmatrix} \boldsymbol{x}_p[i] \\ \boldsymbol{x}_d[i] \\ \boldsymbol{e}_v[i] \end{bmatrix}.$$

Because full row rank of the matrix $\tilde{\boldsymbol{B}}_{pk}$ can be assured [15], $\boldsymbol{F}_d$ can be selected so as to the (1,2) element of the above equation becomes zero for all $k = 1, \cdots, M$.

$$\tilde{\boldsymbol{A}}_{pdk} + \tilde{\boldsymbol{B}}_{pk}\boldsymbol{F}_d = \boldsymbol{O} \tag{29}$$

The simultaneous equation of (29) for all k becomes

$$\tilde{\boldsymbol{A}}_{pd} + \tilde{\boldsymbol{B}}_p\boldsymbol{F}_d = \boldsymbol{O}, \tag{30}$$

$$[\ \tilde{\boldsymbol{A}}_{pd}\ |\ \tilde{\boldsymbol{B}}_p\ ] \triangleq \left[\begin{array}{c|c} \tilde{\boldsymbol{A}}_{pd1} & \tilde{\boldsymbol{B}}_{p1} \\ \vdots & \vdots \\ \tilde{\boldsymbol{A}}_{pdM} & \tilde{\boldsymbol{B}}_{pM} \end{array}\right]. \tag{31}$$

From (30), $\boldsymbol{F}_d$ is obtained by

$$\boldsymbol{F}_d = -\tilde{\boldsymbol{B}}_p^{-1}\tilde{\boldsymbol{A}}_{pd}. \tag{32}$$

On (28) and (29), the influence from disturbance $\boldsymbol{x}_d[i]$ to the inter-sample state $\boldsymbol{x}_p[i+\nu_k]$ at $t = (i+\nu_k)T_f$ can become zero. Moreover, $\boldsymbol{x}_p[i]$, $\boldsymbol{e}_v[i]$ on the sampling point converge to zero at the rate of the eigenvalues of $\tilde{\boldsymbol{A}}_{pM} + \tilde{\boldsymbol{B}}_{pM}\boldsymbol{F}_p$ and $\hat{\boldsymbol{A}}$ (the poles of the regulator and observer). Therefore, the perfect disturbance rejection is achieved ($\boldsymbol{x}_p[i+\nu_k] = 0$) in the steady state. The poles of the regulator and observer will be tuned by the tradeoff between the performance and stability robustness.

Substituting (24) for (26), the feedback type controller is obtained by

$$\begin{bmatrix} \hat{v}[i+1] \\ u[i] \end{bmatrix} = \begin{bmatrix} \hat{A}+\hat{J}F\hat{C} & \hat{b}+\hat{J}F\hat{d} \\ F\hat{C} & F\hat{d} \end{bmatrix} \begin{bmatrix} \hat{v}[i] \\ y[i] \end{bmatrix}. \tag{33}$$

F_p design by the inter-sample observer: In this section, the inter-sample observer is introduced, and the state-feedback control input $F_p\hat{x}_p[i]$ in (26) is decided by the proposed observer. From the estimated state (25) on the sampling points, the inter-sample plant state is estimated by

$$\hat{\tilde{x}}_p[i] = \tilde{A}_p\hat{x}_p[i] + \tilde{B}_p u[i], \tag{34}$$

where $\hat{\tilde{x}}_p[i] = [\hat{x}_p[i+\mu_0], \cdots, \hat{x}_p[i+\mu_{N-1}]]^T$, and $\tilde{A}_p, \tilde{B}_p$ are calculated by (6). Utilizing the inter-sample estimated state, let the state-feedback control input be

$$u_j[i] = f_0\hat{x}_p[i+\mu_{j-1}], \tag{35}$$

where f_0 is the state-feedback gain designed for the plant discretized on T_u. (35) can be described by

$$u[i] = F_0\hat{\tilde{x}}_p[i], \quad F_0 \triangleq diag\{f_0, \cdots, f_0\} \tag{36}$$

From (34) and (36), F_p is given by

$$F_p = (I - F_0\tilde{B}_p)^{-1}F_0\tilde{A}_p. \tag{37}$$

3 Applications to HDD

In the head-positioning control of hard disk drives, the track-seeking mode and the following mode are required. In the track-seeking mode, the feedforward performance is important because the head is moved to the desired track as soon as possible. After that, the head need to be positioned on the desired track while the information is read or written. In the track-following mode, the disturbance rejection performance is important because the head must be positioned finely on the desired track under the vibrations generated by the disk rotation and disturbance [17].

In this section, the proposed TDOF controllers are applied to each modes. While servo signals are detected at a constant period about 100 [μs], the control input can be changed 2~4 times between one sampling period in the recent hardware [3, 4]. Therefore, the proposed approaches are applicable.

3.1 Modeling of the plant

The experimental setup is 3.5-in hard disk drive. Let the nominal model of this plant be

$$P_c(s) = \frac{K_f}{M_p s^2}. \tag{38}$$

The sampling time of this drive is $T_y = T_s = 138.54$ [μs]. The actual plant has the first mechanical resonance mode around 2.7 [kHz]. The Nyquist frequency is also 3.6 [kHz]. In spite of those, this experiment challenges 3 sampling time (2.4 [kHz]) for one track seeking.

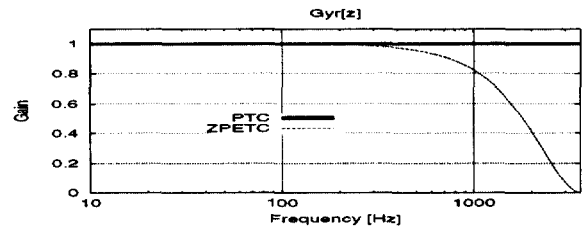

Figure 6: Command responses

3.2 Applications of perfect tracking controller to seeking mode

In this section, the perfect tracking control system proposed in section 2.2 is applied to the seeking mode.

The perfect tracking controller is designed on input multiplicity $N = 4$. Because the plant is second order system ($n = 2$), the perfect tracking is assured $N/n = 2$ times at every sampling points. In the following simulations and experiments, the proposed method is compared with ZPETC proposed in [7]. ZPETC is one of the most popular and important feedforward controllers in the mechanical system control. [4] applied it to the hard disk drive control.

The frequency responses from the desired trajectory $y_d[i]$ to the output $y[i]$ are shown in Fig. 6. Because the proposed method (PTC) assures the perfect tracking, the command response becomes 1 in the all frequency. However, the gain of ZPETC decreases in the high frequency. The frequency of the short-span seeking is 2 [kHz] around. Therefore, it is expected that the proposed method can demonstrate better seeking performance than ZPETC.

The control period T_u of ZPETC becomes four times as long as that of the proposed method because ZPETC is single-rate[1]. The single-rate PI-Lead filter is designed for feedback controller. Moreover, the desired trajectory (39) is selected, which jurk (differential acceleration) is smooth in order not to excite the mechanical resonance mode.

$$y^*(s) = \frac{A_r}{s(\tau_r s+1)^4} \tag{39}$$

In (39), the moving distance is $A_r = 1$[trk] and the frequency is $f_r = \frac{1}{2\pi\tau_r} = 2.8$[kHz].

Simulated and experimental results are shown in Fig. 7. Fig. 7(a)(b) show that the proposed method gives better performance than ZPETC. While the response of ZPETC has large tracking error caused by the unstable zero, that of the proposed method has almost zero tracking error. Fig. 7(c) also indicates that the proposed multirate input is very smooth. Table 1 shows the average seeking-time which obtained in the experiments. The seeking-time of the PTC is much

[1] [4, 18] attempt to extend ZPETC to multirate controllers.

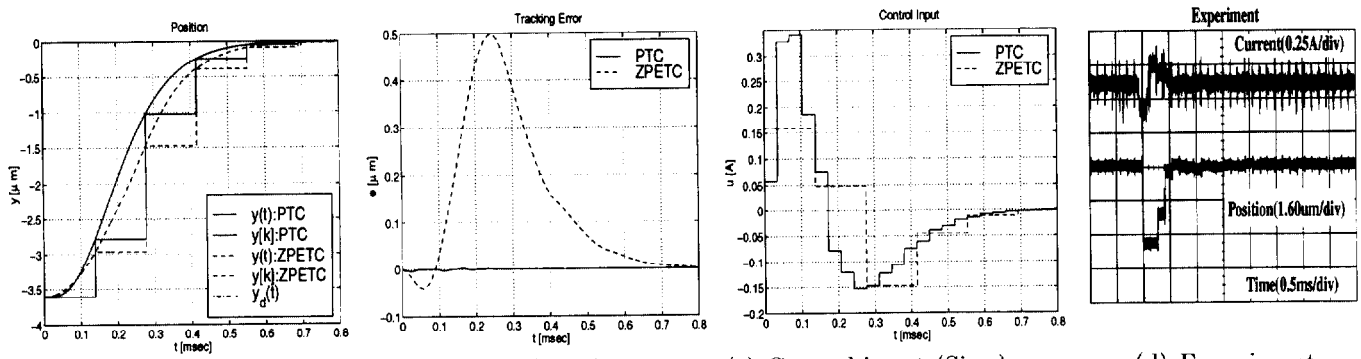

(a) Position (Sim.) (b) Error (Sim.) (c) Control input (Sim.) (d) Experiment

Figure 7: Simulated and experimental results on the seeking mode.

Table 1: Experimental seeking-time.

PTC	ZPETC	Conventional
$3.17T_s$	$3.77T_s$	$4.14T_s$

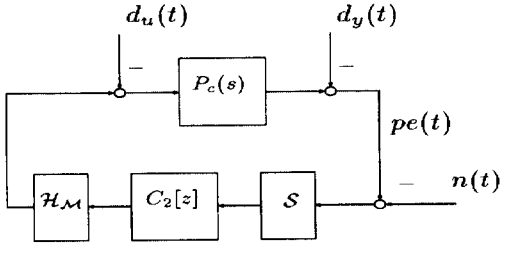

Figure 8: Following mode.

smaller than that of ZPETC and the conventional settling control[17]. The details of this experiments are presented in [19] which includes the middle-span seeking.

3.3 Applications of perfect disturbance rejection controller to following mode

In this section, the perfect disturbance rejection control system proposed in section 2.3 is applied to the following mode. The block diagram of the following mode is shown in Fig. 8. The disturbance $d_y(t)$ represents the vibration of the track generated by the disk rotation, which is called track runout. The objective of this mode is to make the position error $pe(t)$ zero. $n(t)$ and $d_u(t)$ represent the measurement noise and acceleration disturbance, respectively.

In the following mode, the two kinds of disturbance should be considered; repeatable and non-repeatable runout. Repeatable runout (RRO) is synchronous with the disk rotation, and non-repeatable runout (NRRO) is not synchronous. There exist three approaches to reject RRO; (1) repetitive control, (2) feedback control based on the internal model principle, and (3) identification and feedforward control. In this paper, the RRO is modeled by a sinusoidal disturbance, and it is perfectly rejected at M inter-sample points in the steady state. Therefore, the proposed approach is in category (2).

In this paper, the following disturbance models are considered.

$$(\mathrm{A}) : d(s) = \frac{1}{s(s^2+\omega_R^2)}, \quad (\mathrm{B}) : d(s) = \frac{1}{s} \tag{40}$$

The model (A) makes the sensitivity function $S(s)$ small in the low frequency and the rotation frequency of the disk $\omega_R(= 2\pi 120)$. The model (B) is introduced for comparisons with conventional PI-lead filter, because the controller which composed of state-feedback and disturbance observer for (B) becomes 2nd order with an integrator.

The perfect disturbance rejection controllers are designed on $N = 2, 4$. The proposed method is compared with the single-rata disturbance observer, in which the disturbance is modeled by $d[z] = Z[d(s)]$.

The all poles of the regulator and observer are assigned to $\exp(-2\pi f_{cl} T_s)$ as shown in Table 2. These poles are selected to set the open-loop 0 dB cross-over to about 500[Hz]. Fig. 9(a) shows the sensitivity and complimentary sensitivity functions $(S[z], T[z])$ for model (A) and (B).

Fig. 9 shows the simulated results under the 120[Hz] sinusoidal runout added from $t = 0$, which amplitude is 1 [trk] = 3.6[μm]. Although the transient position errors are large, the steady state position errors of the controllers (A) become zero at sampling point, because the feedback controller has the internal model of the RRO. However, Fig. 9(b) shows that the inter-sample responses have the tracking error even in the steady state. It is shown that the errors of the plant position and velocity become zero at every $2T_s/N$ by the proposed controllers. Moreover, the inter-sample posi-

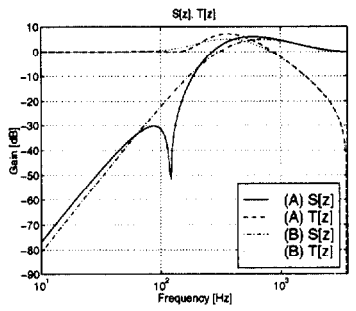

(a) $S[z], T[z] : N = 1$

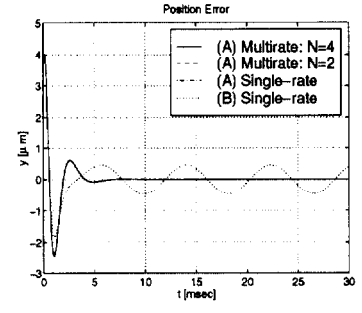

(b) Control input

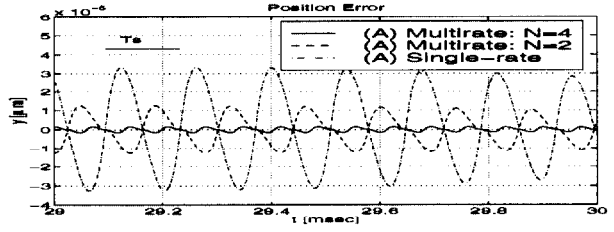

(c) Position error in steady state

Figure 9: Simulated results on the following mode

Table 2: The open loop characteristics.

Disturbance Model	A	A	B	B
Input multiplicity N	1	4	1	4
Closed-loop poles f_{cl}	240	240	390	390
Gain margin [dB]	-6.93	-6.95	11.9	12.5
180 deg cross-over [Hz]	249	249	1573	1635
Phase margin [deg]	29.5	29.6	35.8	36.2
0 dB cross-over [Hz]	507	510	505	506

tion errors of the proposed multirate methods are much smaller than that of the single-rate controller.

The open loop characteristics are shown in Table 2. As same as the results of [1], it is shown that the gain and phase margin are increased by the multirate feedback using the proposed inter-sample observer.

4 Conclusion

In this paper, the digital control systems which have hardware restrictions of $T_u < T_y$ are assumed, the multirate feedforward controller is proposed, which assures the perfect tracking at M inter-sample points. Moreover, the multirate feedback controller is also proposed, which guarantees the perfect disturbance rejection at M inter-sample points at the steady state.

Furthermore, the former is applied to the track-seeking mode of the hard disk drive, and the later is also applied to the track-following mode. The advantages of this approach are demonstrated by the simulations and experiments. The proposed methods can be extended to the plants with time delay [19].

Finally, the authors would like to note that part of this research is carried out with a subsidy of the Scientific Research Fund of the Ministry of Education.

References

[1] W.-W. Chiang, "Multirate state-space digital controller for sector servo systems," in *Conf. Decision Contr.*, pp. 1902–1907, 1990.

[2] A. M. Phillips and M. Tomizuka, "Multirate estimation and control under time-varying data sampling with application to information storage devices," in *Amer. Control Conf.*, pp. 4151–4155, 1995.

[3] S. Takakura, "Design of the tracking system using N-Delay two-degree-of-freedom control and its application to hard disk drives," in *IEEE Conf. Control Applications*, pp. 170–175, August 1999.

[4] M. Kobayashi, T. Yamaguchi, I. Oshimi, Y. Soyama, Y. Hara, and H. Hirai, "Multirate zero phase error feedforward control for magnetic disk drives," in *JSME, IIP '98*, pp. 21–22, August 1998. (in Japanese).

[5] T. Chen and B. Francis, *Optimal Sampled-Data Control Systems*. Springer, 1995.

[6] H. Fujimoto, A. Kawamura, and M. Tomizuka, "Generalized digital redesign method for linear feedback system based on N-delay control," *IEEE/ASME Trans. Mechatronics*, vol. 4, no. 2, pp. 101–109, 1999.

[7] M. Tomizuka, "Zero phase error tracking algorithm for digital control," *ASME, J. Dynam. Syst., Measur., and Contr.*, vol. 109, pp. 65–68, March 1987.

[8] K. J. Åström, P. Hangander, and J. Sternby, "Zeros of sampled system," *Automatica*, vol. 20, no. 1, pp. 31–38, 1984.

[9] P. T. Kabamba, "Control of linear systems using generalized sampled-data hold functions," *IEEE Trans. Automat. Contr.*, vol. 32, no. 9, pp. 772–783, 1987.

[10] T. Mita, Y. Chida, Y. Kazu, and H. Numasato, "Two-delay robust digital control and its applications – avoiding the problem on unstable limiting zeros," *IEEE Trans. AC*, vol. 35, no. 8, pp. 962–970, 1990.

[11] K. L. Moore, S. P. Bhattacharyya, and M. Dahleh, "Capabilities and limitations of multirate control schemes," *Automatica*, vol. 29, no. 4, pp. 941–951, 1993.

[12] H. Fujimoto and A. Kawamura, "Perfect tracking digital motion control based on two-degree-of-freedom multirate feedforward control," in *IEEE Int. Workshop Advanced Motion Control*, pp. 322–327, June 1998.

[13] H. Fujimoto, Y. Hori, and A. Kawamura, "High performance perfect tracking control based on multirate feedforward / feedback controllers with generalized sampling periods," in *14th IFAC World Congress*, vol. C, pp. 61–66, July 1999.

[14] K. Zhou, J. Doyle, and K. Glover, *Robust and Optimal Control*. Prentice-Hall, Inc, 1996.

[15] M. Araki and T. Hagiwara, "Pole assignment by multirate-data output feedback," *Int. J. Control*, vol. 44, no. 6, pp. 1661–1673, 1986.

[16] T. Sugie and T. Yoshikawa, "General solution of robust tracking problem in two-degree-of-freedom control systems," *IEEE Trans. Automat. Contr.*, vol. 31, no. 6, pp. 552–554, 1986.

[17] T. Yamaguchi, H. Numasato, and H. Hirai, "A mode-switching control for motion control and its application to disk drives: Design of optimal mode-switching conditions," *IEEE/ASME Trans. Mechatronics*, vol. 3, no. 3, pp. 202–209, 1998.

[18] Y. Gu and M. Tomizuka, "High performance tracking control system under measurement constraints by multirate control," in *14th IFAC World Congress*, vol. C, pp. 67–71, July 1999.

[19] H. Fujimoto, Y. Hori, T. Yamaguchi, and S. Nakagawa, "Seeking control of hard disk drives by perfect tracking using multirate sampling control," in *IEE of Japan, JIASC '99*, vol. 3, pp. 535–540, August 1999. (in Japanese).